

Gas-Phase Study of the Elementary Reaction of the D1-Ethynyl Radical (C_2D ; $X^2\Sigma^+$) with Propylene (C_3H_6 ; X^1A') under Single-Collision Conditions

Published as part of *The Journal of Physical Chemistry virtual special issue "10 Years of the ACS PHYS Astrochemistry Subdivision"*.

Shane J. Goettl, Chao He, Dababrata Paul, Anatoliy A. Nikolayev, Valeriy N. Azyazov, Alexander M. Mebel, and Ralf I. Kaiser*

 Cite This: *J. Phys. Chem. A* 2022, 126, 1889–1898

 Read Online

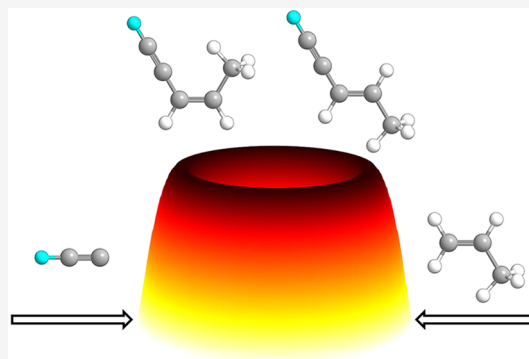
ACCESS |

 Metrics & More

 Article Recommendations

 Supporting Information

ABSTRACT: The bimolecular gas-phase reactions of the D1-ethynyl radical (C_2D ; $X^2\Sigma^+$) with propylene (C_3H_6 ; X^1A') and partially substituted D3–3,3,3-propylene ($C_2H_3CD_3$; X^1A') were studied under single collision conditions utilizing the crossed molecular beams technique. Combining our laboratory data with electronic structure and statistical calculations, the D1-ethynyl radical is found to add without barrier to the C1 and C2 carbons of the propylene reactant, resulting in doublet C_5H_6D intermediate(s) with lifetime(s) longer than their rotational period(s). These intermediates undergo isomerization and unimolecular decomposition via atomic hydrogen loss through tight exit transition states forming predominantly *cis/trans*-3-penten-1-yne ((HCC)CH=CH(CH₃)) and, to a minor amount, 3-methyl-3-buten-1-yne ((HCC)C(CH₃)=CH₂) via overall exoergic reactions. Although the title reaction does not lead to the cyclopentadiene molecule (*c*- C_5H_6 , X^1A_1), high-temperature environments can convert the identified acyclic C_5H_6 isomers through hydrogen atom assisted isomerization to cyclopentadiene (*c*- C_5H_6 , X^1A_1). Since both the ethynyl radical and propylene reactants have been observed in cold interstellar environments such as TMC-1 and the reaction is exoergic and all barriers lie below the energy of the separated reactants, these C_5H_6 product isomers are predicted to form in those low-temperature regions.



1. INTRODUCTION

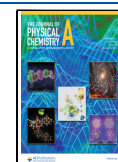
The ethynyl radical (C_2H , $X^2\Sigma^+$) has been recognized by the astrochemistry and planetary science community^{1–3} as a fundamental building block involved in low-temperature molecular mass growth processes leading to highly unsaturated hydrocarbons—among them, aromatic structures such as *o*-benzynes (*o*- C_6H_4 , X^1A_1),^{4,5} benzene (C_6H_6 , X^1A_{1g}),⁶ and toluene ($C_6H_5CH_3$, X^1A')⁷ (Scheme 1), along with polyacetylenes such as diacetylene (C_4H_2 , $X^1\Sigma_g^+$)⁸ and triacetylene (C_6H_2 , $X^1\Sigma_g^+$)⁹ in cold molecular clouds such as the Taurus Molecular Cloud (TMC-1)⁶ and in hydrocarbon rich atmospheres of planets and their moons such as Titan and Triton.¹⁰ In the interstellar medium (ISM), the ethynyl radical was detected in 1974 by Thaddeus and co-workers¹¹ toward the Orion Molecular Cloud (OMC-1) possibly formed via photodissociation of acetylene (C_2H_2 , $X^1\Sigma_g^+$)¹² or via the barrierless and exoergic bimolecular reactions of ground-state carbon (C , 3P) with triplet carbene (CH_2 , X^3B_1) or the methylidyne (CH , $X^2\Pi$) radical self-reaction. In hydrocarbon rich atmospheres, solar Lyman- α photons photodissociate acetylene (C_2H_2 , $X^1\Sigma_g^+$) to ethynyl (C_2H , $X^2\Sigma^+$) followed by

rapid, barrierless reactions with unsaturated hydrocarbons through stepwise two-carbon molecular mass growth processes holding rate constants of a few 10^{-10} $cm^3 s^{-1}$, even at temperatures as low as 15 K.¹³ Crossed molecular beam studies merged with electronic structure calculations provided knowledge of a rich hydrocarbon chemistry of elementary reactions of ethynyl radicals with unsaturated C_2 to C_8 hydrocarbons with reaction mechanisms ranging from simple ethynyl addition–hydrogen atom elimination pathways along with a conservation of the carbon moieties to unprecedented addition–cyclization pathways leading to aromatic structures such as *o*-benzynes (*o*- C_6H_4 , X^1A_1),^{4,5} benzene (C_6H_6 , X^1A_{1g}),⁶ and toluene ($C_6H_5CH_3$, X^1A')⁷ (Scheme 1).

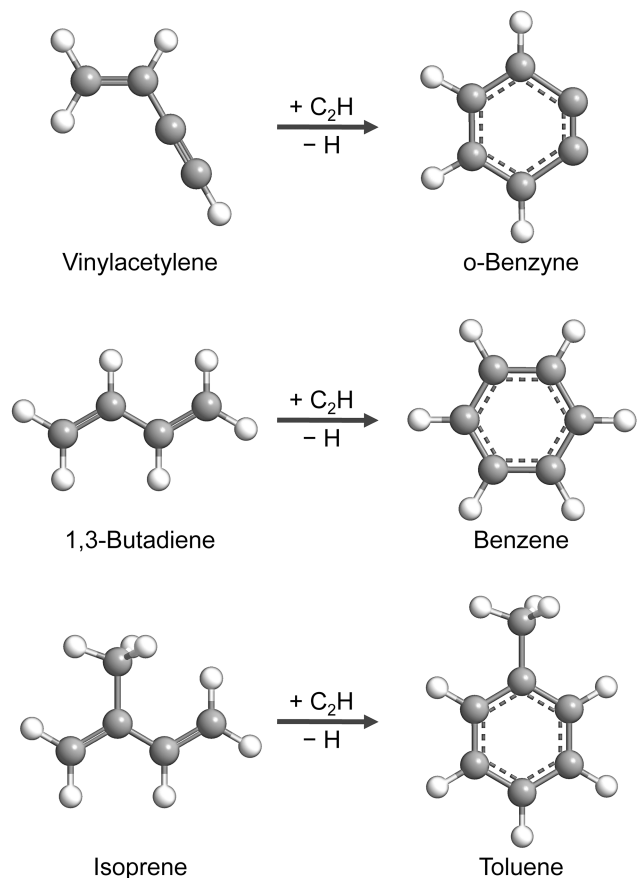
Received: January 13, 2022

Revised: March 1, 2022

Published: March 15, 2022



Scheme 1. Addition–Cyclization Reaction Pathways Involving Key Reactions of the Ethynyl Radical with Vinylacetylene, 1,3-Butadiene, and Isoprene, Leading to *o*-Benzyne, Benzene, and Toluene, Respectively



Surprisingly, the elementary reaction of the ethynyl radical with propylene (C_3H_6), as detected in the cold molecular cloud TMC-1¹⁴ and in Titan's atmosphere,¹⁵ has not been explored to date under single collision conditions. This system accesses the doublet C_5H_7 potential energy surface (PES) and hence may lead to C_5H_6 isomers, among them the cyclopentadiene molecule ($c-C_5H_6$, X^1A_1), which was recently observed toward the molecular cloud TMC-1.¹⁶ Here, we reveal the chemical dynamics of the elementary reaction of the D1-ethynyl radical (C_2D , $X^2\Sigma^+$) with propylene (C_3H_6 , X^1A'), along with its partially D3-deuterated counterpart ($C_2H_3CD_3$; X^1A'). Combined with electronic structure calculations, the results propose the formation of partially deuterated *cis/trans*-3-penten-1-yne ((HCC)CH=CH(CH₃)) and 3-methyl-3-buten-1-yne ((HCC)C(CH₃)=CH₂) products through long-lived intermediates initiated by D1-ethynyl radical addition to the α -carbon of propylene; these dynamics are also compared to the isoelectronic cyano (CN, $X^2\Sigma^+$)–propylene (C_3H_6 , X^1A') system studied earlier in our group.¹⁷ Although the title reaction does not lead to the cyclopentadiene molecule ($c-C_5H_6$, X^1A_1), in high-temperature environments such as circumstellar envelopes of carbon stars like IRC+10216 close to the central star and planetary nebulae as their descendants along with combustion systems, hydrogen-atom-assisted isomerization processes could convert the identified acyclic C_5H_6 isomers *cis/trans*-3-penten-1-yne and 3-methyl-3-buten-1-yne to cyclopentadiene ($c-C_5H_6$, X^1A_1), but not in cold

molecular clouds, where the addition of atomic hydrogen to double and triple bonds is hindered by barriers of up to 30 kJ mol⁻¹ due to the low temperatures of 10 K.

2. METHODS

2.1. Experimental Methods. Reactions of the D1-ethynyl radical (C_2D , $X^2\Sigma^+$) with propylene (C_3H_6 , $\geq 99\%$, Sigma–Aldrich) and of D3–3,3,3-propylene ($C_2H_3CD_3$, 99.8% D atom, CDN Isotopes) were performed under single collision conditions utilizing a crossed molecular beams apparatus.^{18–28} Briefly, a pulsed supersonic beam of D1-ethynyl radicals was generated by laser ablation of a rotating carbon rod with 5–7 mJ of the 266 nm output of a Nd:YAG laser (Quanta-Ray Pro 270, Spectra-Physics); the ablated species subsequently reacted with neat deuterium gas (D_2 , 99.999%, Linde), which passed through a Proch-Trickl²⁹ pulsed valve with an open time of 80 μ s at an amplitude of -400 V. Deuterium also acted as a carrier gas with a backing pressure of 4 atm.^{4,6,7,30,31} The pulsed beam passed through a skimmer and the velocity was selected by a chopper wheel resulting in a peak velocity (v_p) of 2136 ± 19 m s⁻¹ and a speed ratio (S) of 5.5 ± 0.3 . Since the travel time of D1-ethynyl radicals from the ablation center to the interaction region was ~ 30 μ s, any species in the $A^2\Pi$ excited state, which has a lifetime of < 1 μ s, relaxed back to the $X^2\Sigma^+$ ground state. The D1-ethynyl beam crossed then perpendicularly with a pulsed propylene beam ($v_p = 840 \pm 10$, $S = 11.0 \pm 0.2$) resulting in a collision energy (E_c) and center-of-mass (CM) angle (Θ_{CM}) of 42.3 ± 0.8 kJ mol⁻¹ and $33.2 \pm 0.5^\circ$, respectively; experiments conducted with D3–3,3,3-propylene ($v_p = 830 \pm 10$ m s⁻¹, $S = 11.0 \pm 0.2$) gave an E_c of 43.3 ± 0.8 kJ mol⁻¹ and Θ_{CM} of $34.7^\circ \pm 0.6^\circ$. It is important to note that the primary beam also contains carbon atoms, as well as dicarbon and tricarbon molecules. Previous experiments involving tricarbon reactions with acetylene, ethylene,³² and methylacetylene³³ suggest a high entrance barrier for the reaction of tricarbon with propylene, thus insinuating it was not observed under our experimental conditions. In addition, carbon and dicarbon are lighter by 14 and 2 amu than D1-ethynyl, respectively, indicating that the products of their reactions with propylene do not interfere with the products of the title reaction.

Reactively scattered products were collected by a triply differentially pumped universal detector, which is rotatable within the plane of the reactant beams. Neutral products are ionized by electron impact ionization at 80 eV and an emission current of 2 mA. Ionized products are filtered by a quadrupole mass spectrometer (QMS) operating in the time-of-flight (TOF) mode at a constant mass-to-charge ratio (m/z). Up to 2.5×10^6 TOF spectra were taken in 2.5° steps at angles between $19^\circ \leq \Theta \leq 49^\circ$, with respect to the D1-ethynyl beam ($\Theta = 0^\circ$). A laboratory angular distribution was created by integrating the TOF spectra and normalizing to the CM angle. To gain information on the reaction dynamics, the laboratory angular distribution and TOF spectra were fit utilizing a forward convolution routine; this created user-defined CM translational energy ($P(E_T)$) and angular ($T(\theta)$) flux distributions, which were refined iteratively until a satisfactory fit of the laboratory data was achieved.^{34,35} These functions were used to develop a flux contour map, shown as $I(u, \theta) \approx P(u) \times T(\theta)$,³⁶ which portrays an overall image of the outcome of the reaction.

2.2. Computational Methods. Geometries of the reactants, products, reaction intermediates, and transition

states on the section of the C_3H_7 PES accessed by the $C_2H + C_3H_6$ reaction were optimized applying the long-range corrected hybrid density functional $\omega B97X-D$ ³⁷ with the 6-311G(d,p) basis set. Vibrational frequencies for each optimized structure were calculated at the same $\omega B97X-D/6-311G(d,p)$ level of theory to assess zero-point vibrational energy corrections (ZPE); the frequencies were also utilized in rate constant computations. Single-point energies for all stationary structures were rectified using the explicitly correlated coupled clusters method with single and double excitations and perturbative treatment of triple excitations, CCSD(T)-F12,^{38,39} with Dunning's correlation-consistent cc-pVTZ-f12 basis set.⁴⁰ The CCSD(T)-F12/cc-pVTZ-f12// $\omega B97X-D/6-311G(d,p) + ZPE(\omega B97X-D/6-311G(d,p))$ dual-level approach is normally capable of achieving accuracy in relative energies within 4 kJ mol⁻¹ or better.⁴¹ The PES calculations were performed with the GAUSSIAN 09⁴² and MOLPRO 2010⁴³ quantum chemistry software packages.

The Rice–Ramsperger–Kassel–Marcus (RRKM) approach^{44–46} was employed to evaluate energy-dependent rate constants of all unimolecular reaction steps, following the initial ethynyl radical addition to propylene. In these calculations, the internal energy for all the C_5H_7 isomers and transition states was taken as the sum of the collision and chemical activation energy, with the latter being a negative of the relative energy of each species, with regard to the separated $C_2H + C_3H_6$ reactants. The internal energy-dependent rate constants were computed using our own Unimol code.⁴⁷ The calculations were performed at the zero-pressure limit emulating the conditions of the crossed molecular beams experiment and those in cold molecular clouds. The computed RRKM rate constants were used to obtain reaction product branching ratios employing the steady-state approximation.⁴⁸

3. RESULTS

3.1. Laboratory Frame. Reactive scattering signal for the reaction of the D1-ethynyl radical (C_2D , $X^2\Sigma^+$, 26 amu) with propylene (C_3H_6 , X^1A' , 42 amu) was observed at $m/z = 67$ ($C_5H_5D^+$) and 66 ($C_5H_4D^+$, $C_5H_6^+$). The TOF spectra obtained at both m/z ratios overlap after scaling suggesting that signal at $m/z = 67$ and 66 originate from the same reaction channel forming the heavy product (C_5H_5D , 67 amu) and atomic hydrogen (H, 1 amu). Signal at $m/z = 66$ is attributed to dissociative ionization of the C_5H_5D product in the electron impact ionizer. The TOF spectra (Figure 1B) for the C_5H_5D product were collected at $m/z = 67$ and are very broad, ranging typically from 480 μs to 820 μs . The laboratory angular distribution (Figure 1A) is almost symmetric around the center of mass angle Θ_{CM} , thus indicating indirect scattering dynamics via C_5H_6D reaction intermediate(s) leading to C_5H_5D plus atomic hydrogen. Therefore, the hydrogen atom is emitted from the propylene reactant.

The reaction of the D1-ethynyl radical (26 amu) with D3-3,3,3-propylene ($C_2H_3CD_3$, X^1A' , 45 amu) was also conducted in order to gain information on the position(s) of atomic hydrogen loss(es), i.e. the methyl group versus the vinyl moiety. Reactive scattering signal for this system was detected at the CM angle of 34° at $m/z = 70$ ($C_5H_2D_4^+$) and 69 ($C_5HD_4^+$, $C_5H_3D_3^+$). The TOF spectra for both $m/z = 70$ and 69 overlap after scaling revealing the likely existence of only one reaction channel, i.e., the atomic hydrogen loss from the vinyl (C_2H_3) moiety; signal at $m/z = 69$ is attributed to dissociative electron impact ionization of $C_5H_2D_4$. This finding

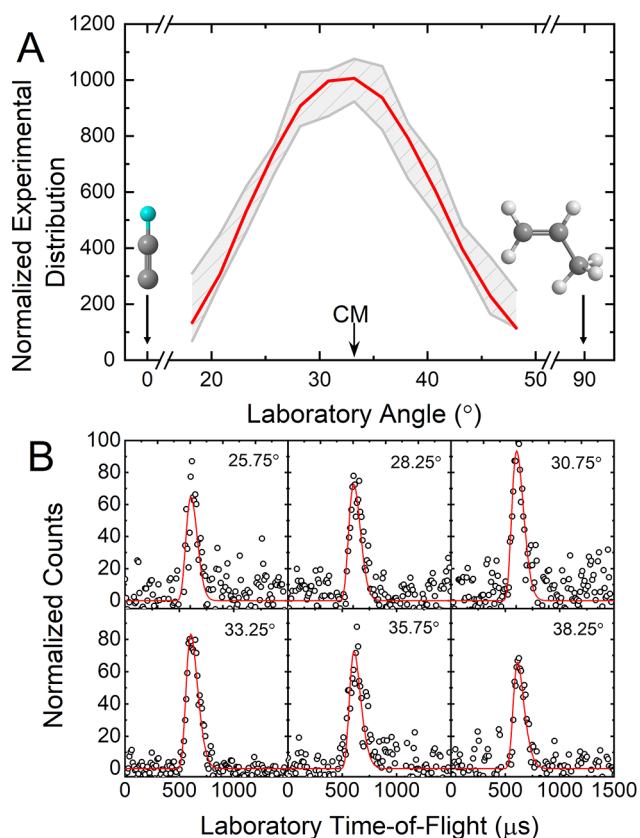


Figure 1. (A) Laboratory angular distribution and (B) time-of-flight (TOF) spectra recorded at mass-to-charge (m/z) = 67 for the reaction of propylene (C_3H_6) with the D1-ethynyl radical (C_2D). CM represents the center-of-mass angle, and 0° and 90° define the directions of the D1-ethynyl and propylene beams, respectively. The black circles depict the data, red lines the fits, and shaded areas the experimental error limits. Atoms are colored as follows: carbon (gray), hydrogen (white), and deuterium (light blue).

reveals that the atomic hydrogen loss occurs at least from the C_1 and/or C_2 carbons of propylene. A comparison of the intensity of the reactive scattering signal at $m/z = 70$ for the D1-ethynyl – D3-3,3,3-propylene system with that at $m/z = 67$ for the D1-ethynyl–propylene system results in a ratio of $(0.8 \pm 0.5):(1.0 \pm 0.4)$, respectively. This indicates that the hydrogen atom loss from the methyl group of propylene is only a minor contributor within the error limits.

3.2. Center of Mass Frame. To elucidate the reaction dynamics of the D1-ethynyl radical with propylene, the laboratory data were transformed from the laboratory reference frame to the CM reference frame. The TOF spectra and laboratory angular distribution were fit with a single channel corresponding to the product C_5H_5D plus atomic hydrogen; the best-fit CM functions are shown in Figure 2. The red lines shown in Figure 1B correspond to the best fits of the data within the error limits specified by Figures 1A and 2, which are represented by gray envelopes. The uniqueness of the TOF fits (Figure 1B) is defined by the range of acceptable fits within these error limits. In addition, any reaction channel other than H loss would have a different mass-to-charge ratio and therefore a different flight time, giving a TOF peak in a different position, which also attests to the uniqueness of the fits for the TOF spectra. The CM translational energy distribution, $P(E_T)$ (Figure 2A), provides a maximum

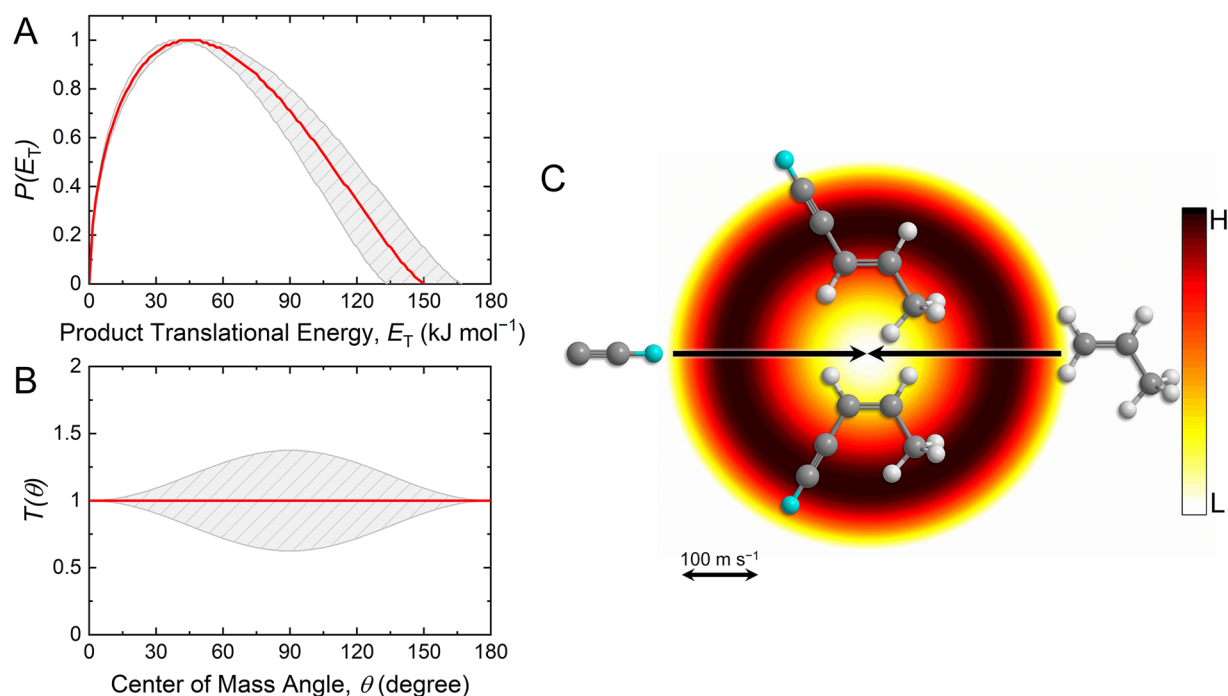


Figure 2. (A) CM translational energy and (B) angular flux distributions, as well as (C) the associated flux contour map, leading to the formation of C_3H_3D isomers plus atomic hydrogen in the reaction of the D1-ethynyl radical (C_2D) with propylene (C_3H_6). Red lines define the best-fit functions while shaded areas provide the error limits. The flux contour map represents the intensity of the reactively scattered products as a function of product velocity (u) and scattering angle (θ), and the color bar indicates flux gradient from high (H) to low (L) intensity. Atoms are colored as follows: carbon (gray), hydrogen (white), and deuterium (light blue).

translational energy release, E_{max} , of 150 ± 17 kJ mol^{-1} . The reaction energy can be recovered using the maximum translational energy and the reaction collision energy, given by $\Delta_r G = E_c - E_{max}$ for those reaction products born without internal excitation. Hence, this reaction is exoergic by 108 ± 18 kJ mol^{-1} . Furthermore, the distribution has a maximum at 45 kJ mol^{-1} , which indicates a tight exit transition state from the decomposing C_3H_6D intermediate(s) to C_3H_3D plus atomic hydrogen.⁴⁹ Finally, the CM angular flux distribution, $T(\theta)$ (Figure 2B), provides additional information on the scattering dynamics. This distribution shows a forward–backward symmetry and equal scattering probability in all directions. These findings suggest indirect scattering dynamics through C_3H_6D intermediate(s) with lifetimes longer than the rotational period(s). The flux contour map as shown in Figure 2C reflects these findings. The isotropic scattering signal is the effect of the light H atom carrying away an insignificant fraction of the total angular momentum.⁵⁰

4. DISCUSSION

The experimental results were combined with electronic structure and statistical calculations to unveil the underlying dynamics of the ethynyl–propylene system (see Figures 3–5 and Table 1, as well as Tables S1–S3 in the Supporting Information). The doublet PES was studied systematically through ethynyl radical addition to either the central or terminal carbon atoms of the carbon–carbon double bond of the propylene molecule, followed by isomerization via 19 C_5H_7 intermediates (i1–i19) and 48 transition states eventually leading to atomic hydrogen loss products (C_5H_6 ; p2, p3, p4, p5, p6, p7, p9), CH_3 loss product (C_4H_4 ; p1), C_2H_3 loss product (C_3H_4 ; p10), and C_3H_3 loss product (C_2H_4 ; p8). For

Table 1. Statistical Branching Ratios for the C_2H + Propylene Reaction at Collision Energies of 41.1 and 0 kJ mol^{-1}

	Branching Ratios (%)		
	i1	i3	i4
$E_c = 41.1 \text{ kJ mol}^{-1}$			
initial intermediate	100	100	100
p1	46.3	34.6	34.7
p2	11.8	15.1	15.1
p3	14.0	17.9	17.9
p4	7.2	9.2	9.2
p5	7.2	9.2	9.2
p6	6.2	7.9	7.9
p7	0.9	1.1	1.1
p8	1.2	1.6	1.6
p9	5.1	3.3	3.2
p10	0.1	0.1	0.1
$E_c = 0 \text{ kJ mol}^{-1}$			
initial intermediate	100%	100%	100%
p1	50.6	46.3	46.3
p2	12.6	14.0	14.0
p3	14.8	16.4	16.4
p4	5.4	6.0	6.0
p5	5.4	6.0	6.0
p6	5.0	5.6	5.6
p7	0.7	0.7	0.7
p8	0.8	0.9	0.9
p9	4.6	4.0	4.0
p10	0.1	0.1	0.1

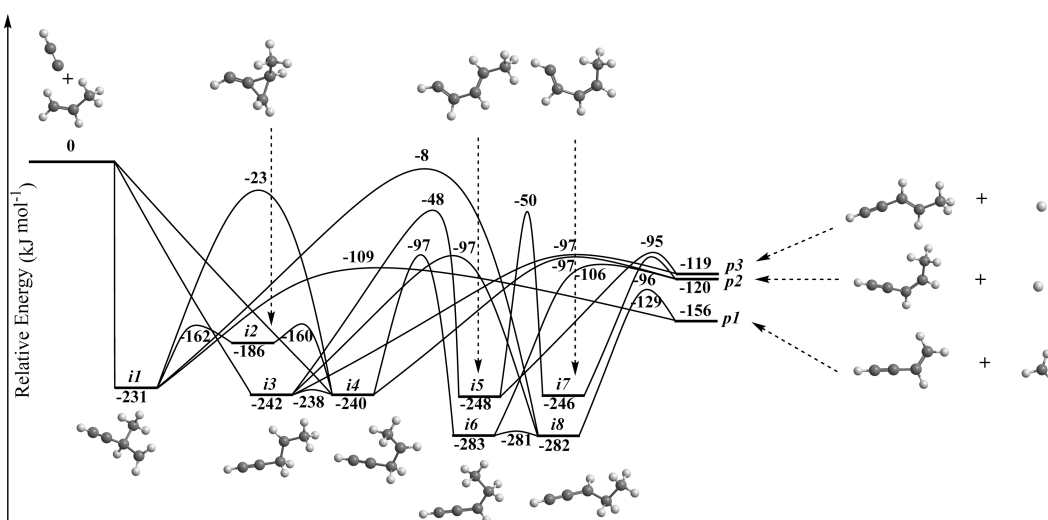


Figure 3. Portion of the C_5H_7 PES leading to products **p1–p3** through intermediates **i1–i8**.

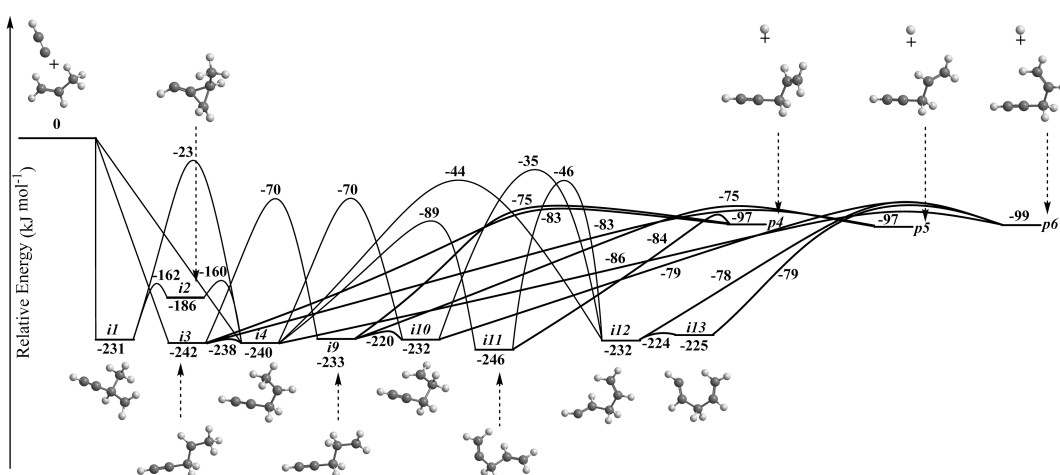


Figure 4. Portion of the C_5H_7 PES leading to products **p4–p6** through intermediates **i1–i4** and **i9–i11**.

simplicity, the PES has been split into three figures (shown in Figures 3–5).

4.1. Formation of Products **p1–p3 through Intermediates **i1–i8**.** The formation of products **p1–p3** through intermediates **i1–i8** is depicted in Figure 3. The radical center of the ethynyl radical can add without barrier to the C1 or C2 carbon atoms of the carbon–carbon double bond of propylene to form three possible intermediates. First, the addition to the central carbon leads to intermediate **i1**; second, addition to the sterically more accessible terminal (C1) carbon leads to *cis* and *trans* conformers **i4** and **i3**, respectively. **i1** can cyclize to **i2**, which then undergoes ring opening forming **i4** via barriers of 16 and 14 kJ mol^{-1} , with respect to **i2**. Essentially, this reaction sequence portrays an ethynyl migration from C2 to C1 via the cyclic intermediate **i2**. Alternatively, **i1** can isomerize to **i4** in one step through ethynyl migration without a formation of the three-membered ring intermediate **i2** through a much higher barrier of 209 kJ mol^{-1} above **i1**. Intermediate **i1** can also experience a methyl group shift from CH to CH_2 through a significant barrier (223 kJ mol^{-1}) above **i1**, producing **i8**. Product **p1** can be formed by methyl loss from **i1** through an exit transition state located 47 kJ mol^{-1} above **p1**. Intermediate **i3** can form **i4** by rotation around the central CH–CH_2 bond

through a small barrier of only 2 kJ mol^{-1} above **i4**. Alternately, **i3** may undergo two distinct hydrogen atom migrations to form **i5** or **i8** through barriers of 194 or 145 kJ mol^{-1} above **i3**, respectively. Product **p3** can be formed by hydrogen atom emission from intermediate **i3** through an exit barrier 22 kJ mol^{-1} above **p3**. **i4** can undergo hydrogen shift to **i6** through a 143 kJ mol^{-1} barrier above **i4**; both **i4** and **i6** can decompose to **p2** through exit barriers of 23 and 14 kJ mol^{-1} above **p2**. Intermediate **i6** can also isomerize through a small barrier of only 1 kJ mol^{-1} by the CH–CH_2 bond rotation to **i8**, which then decomposes to **p1** through an exit transition state 27 kJ mol^{-1} above **p1**. **i5** may form **i7** via a central C=C bond rotation through a high barrier of 196 kJ mol^{-1} above **i7**; both **i5** and **i7** can decompose by hydrogen loss, forming **p3** and **p2**, respectively, through barriers 24 kJ mol^{-1} above their respective products.

4.2. Formation of Products **p4–p6 through Intermediates **i1–i4** and **i9–i13**.** The formation of products **p4–p6** through intermediates **i1–i4** and **i9–i13** is depicted in Figure 4. The reactions portraying the section of the PES, which compiles the pathways to products **p4–p6**, are initiated by the same entrance channels as those shown in Figure 3 and discussed in 4.1. Intermediate **i3** can isomerize by hydrogen

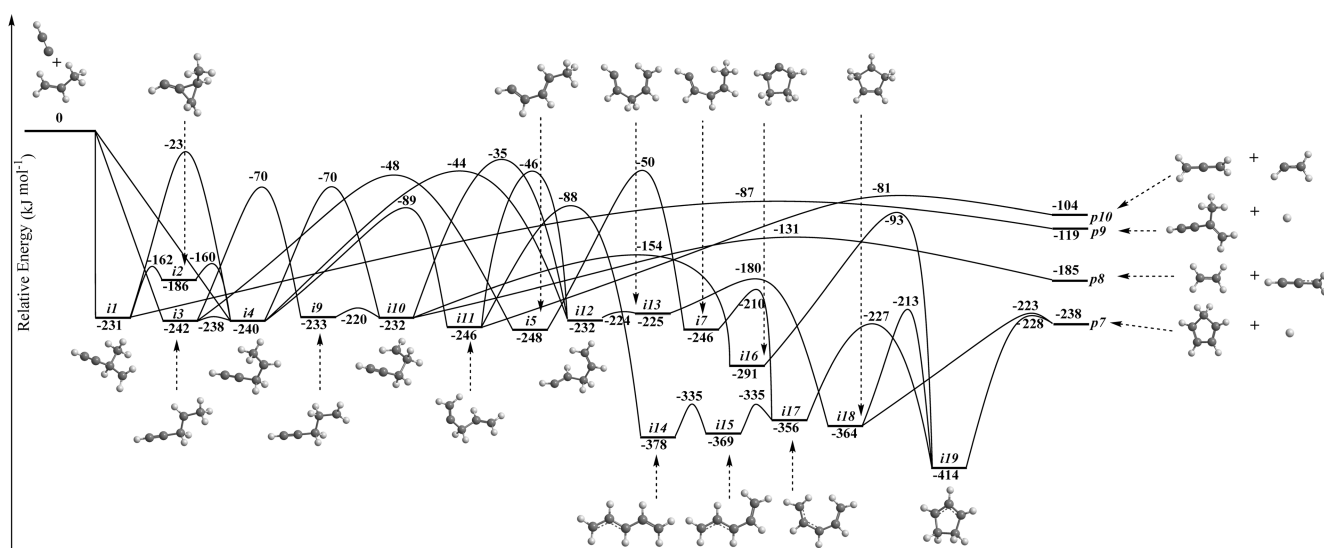


Figure 5. Portion of the C_5H_7 PES leading to products $p7$ – $p10$ through intermediates $i1$ – $i5$, $i7$, and $i9$ – $i19$.

atom migration from the methyl group to form $i9$ through a barrier located 163 kJ mol^{-1} above $i9$. In addition, $i3$ may decompose via atomic hydrogen loss from the methyl group to produce $p4$ or $p5$. From $i4$, intermediates $i10$ – $i12$ can be formed via distinct hydrogen atom migrations, as well as product $p6$ by atomic hydrogen loss, through barriers of 170, 151, 196, and 154 kJ mol^{-1} above $i4$, respectively. Intermediate $i9$ may undergo bond rotation to $i10$ through a 13 kJ mol^{-1} barrier or decomposes to form $p5$ by hydrogen atom loss over an exit barrier of 22 kJ mol^{-1} above the products. The decomposition of $i10$ leads to $p6 + H$ through an exit transition state positioned 20 kJ mol^{-1} above $p6$. Both $i10$ and $i11$ can undergo hydrogen shifts to $i12$ through significant barriers located 197 and 186 kJ mol^{-1} , respectively, above $i12$. Alternately, $i11$ may decompose by hydrogen loss to $p4$ via a small exit barrier 13 kJ mol^{-1} above the product. Finally, $i12$ can form $i13$ via bond rotation through a 1 kJ mol^{-1} barrier; both $i12$ and $i13$ can form $p6$ via hydrogen loss decomposition through exit transition states 21 and 20 kJ mol^{-1} above $p6$. All three products in this section of the surface lie within the limits of the experimentally derived reaction energy; $p4$ and $p5$ can be formed through loose exit barriers immediately from $i3$, while $p6$ can be produced from the decomposition of $i4$, where both intermediates are created from the barrierless addition of the reactants. Essentially, $p4$ – $p6$ represent distinct conformers formed via hydrogen atom elimination defacto from the methyl group of the propylene moiety.

4.3. Formation of Products $p7$ – $p10$ through Intermediates $i1$ – $i5$, $i7$, and $i9$ – $i19$. Figure 5 depicts the formation of products $p7$ – $p10$ through intermediates $i1$ – $i5$, $i7$, and $i9$ – $i19$. Products $p8$ – $p10$ are formed from $i10$, $i1$, and $i11$ by C_3H_3 , H atom, and C_2H_3 loss through exit transition states located 54 , 32 , and 23 kJ mol^{-1} above the products, respectively. The formation of cyclopentadiene ($p7$) involves multiple steps. Intermediate $i10$ can undergo ring closure to form $i16$, passing a barrier located 78 kJ mol^{-1} above $i10$. This is followed by hydrogen atom migration to $i19$ through a transition state located 198 kJ mol^{-1} above $i16$. $i11$ can form $i14$ via a hydrogen migration barrier of 158 kJ mol^{-1} above $i11$ prior to conformational isomerization through barriers of 43 and 34 kJ mol^{-1} to $i15$ and then to $i17$. Intermediate $i17$ can

also be formed by 1,5-hydrogen migration from $i7$ through a low 36 kJ mol^{-1} barrier above $i7$. $i13$ can undergo ring closure to form $i18$ through a barrier of 45 kJ mol^{-1} . Intermediate $i18$ can decompose to $p7$ via hydrogen loss through a loose transition state residing 15 kJ mol^{-1} above $p7$. Both $i17$ and $i18$ can isomerize to $i19$ via ring closure and hydrogen migration, respectively, through barriers located 129 kJ mol^{-1} above $i17$ and 151 kJ mol^{-1} above $i18$. Intermediate $i19$ can decompose to $p7$ through an exit transition state lying 10 kJ mol^{-1} above $p7$. In the $p7$ – $p10$ group, products $p9$ and $p10$ match the experimentally derived reaction energy with only the former decomposing via hydrogen atom loss. Product $p9$ is formed from a single reaction pathway that involves an ethynyl addition–hydrogen loss and a fairly low exit barrier of only 32 kJ mol^{-1} .

4.4. Reaction Pathways. The experimental results are now linked with the computations to propose the most likely reaction pathways. *First*, the laboratory data of the D1-ethynyl (C_2D)–propylene (C_3H_6) system reveal the formation of C_5H_5D products via atomic hydrogen loss at a collision energy of $42.3 \pm 0.8 \text{ kJ mol}^{-1}$. The nearly symmetric laboratory angular distribution indicates an indirect reaction through C_5H_6D reaction intermediate(s) with the hydrogen atom leaving from the propylene molecule. *Second*, the D1-ethynyl reaction with D3–3,3,3-propylene provides evidence that hydrogen atom loss occurs dominantly from the C1 and/or C2 carbons of the vinyl moiety. *Third*, from the $P(E_T)$, the reaction energy is derived to be $-108 \pm 18 \text{ kJ mol}^{-1}$; the distribution maximum of 45 kJ mol^{-1} indicates a tight exit transition state(s). The isotropic $T(\theta)$ denotes an indirect reaction with long-lived intermediate(s).

The computations predict three barrierless additions of the ethynyl radical with its radical center located at the C atom to the C1 and/or C2 carbon of propylene forming intermediates $i1$, $i3$, and/or $i4$ (recall Figures 3–5). Overall, 19 intermediates are accessible through isomerization; these were found to undergo unimolecular decomposition to 10 possible products $p1$ – $p10$ with reaction energies ranging from 97 kJ mol^{-1} to 238 kJ mol^{-1} . In principle, all reaction intermediates are energetically accessible, since their energies and the transition states connecting them lie below the collision energy of $42.3 \pm$

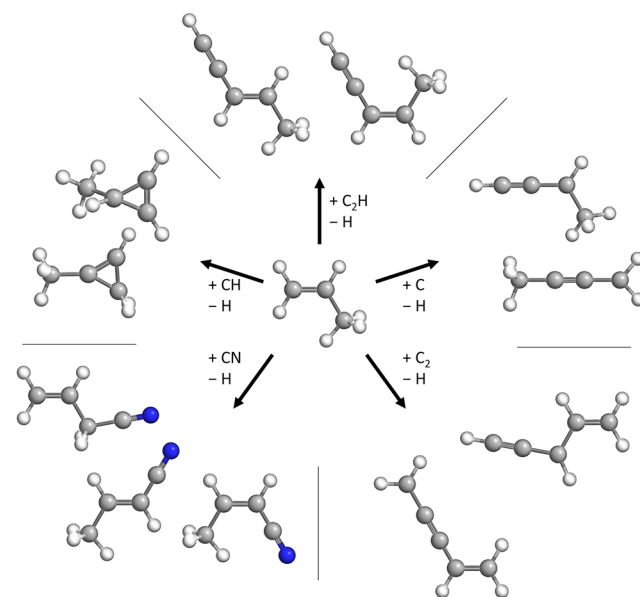
0.8 kJ mol⁻¹. These possible pathways are narrowed down by comparing the experimental reaction energy of -108 ± 18 kJ mol⁻¹ with the computed reaction energies. This comparison suggests that, based on the energetics, **p2–p6** and **p9** ($\Delta_R G = -120, -119, -97, -97, -99,$ and -119 kJ mol⁻¹) can account for the experimental reaction energy, within the error limits. Only accounting for the hydrogen loss products, **p10** (-104 kJ mol⁻¹), which involves the formation of allene (H₂CCCH₂) through loss of a vinyl radical (C₂H₃), can be eliminated. Since the position of the hydrogen atom loss in the unimolecular decomposition of the C₃H₇ intermediates was found to predominantly stem from the vinyl moiety (i.e., no hydrogen loss from the methyl group), the 4-penten-1-yne isomers (**p4–p6**) cannot form since they would involve a hydrogen atom elimination in intermediate **i3** and/or **i4** from the methyl group. However, the remaining products **p2**, **p3**, and **p9** are accessible via unimolecular decomposition from collision complexes **i1**, **i3**, and/or **i4**. Also, the PES reveals that pathways to **p4–p6** have slightly higher energy exit transition states than those leading to **p2**, **p3**, and **p9**, with the lowest values of $-84, -75,$ and -70 kJ mol⁻¹, with respect to the separated reactants for **p4**, **p5**, and **p6**, respectively, as compared to $-97, -97,$ and -87 kJ mol⁻¹ for **p2**, **p3**, and **p9**, respectively. Therefore, due to the higher energy barriers, 4-penten-1-yne isomers (**p4–p6**) are deemed less likely to form; consequently, these considerations propose that 3-penten-1-yne isomers (**p2/p3**) and 3-methyl-3-buten-1-yne (**p9**) likely represent the major reaction products. The most probable reaction pathways to form **p2** and **p3** involve barrierless ethynyl addition to the C1 carbon of propylene to form **i4** and **i3**, which undergo H-atom loss through tight exit transition states of 23 and 22 kJ mol⁻¹ above the separated products, respectively. **p9** is formed by barrierless ethynyl addition to the more sterically hindered C2 carbon of propylene to form **i1** prior to a hydrogen atom loss also through a tight exit transition state of 32 kJ mol⁻¹ above the separated products. In all three cases, unimolecular decomposition occurs in one step after the formation of the collision complex.

RRKM calculations provide statistical branching ratios for the reaction of ethynyl radicals with propylene within a limit of a complete energy randomization. Three distinct sets of calculations are formed starting with intermediates **i1**, **i3**, and **i4**, respectively, for the experimental collision energy and for zero collision energy resembling the low temperature (10 K) conditions of molecular clouds such as TMC-1 and OMC-1 (Table 1). The most likely reaction pathway involves methyl loss leading to vinylacetylene (**p1**) at 35%–46% of the reaction products formed; however, this pathway could not be explored experimentally because the D1-ethynyl (C₂D, X²Σ⁺) beam contains atomic carbon (C; ³P_j), which reacts with propylene (C₃H₆; X¹A') to form the methylpropargyl radical (C₄H₅) via H-atom loss.⁵¹ This product can fragment within the ionizer to C₄H₄⁺ ions at *m/z* = 52, cloaking any signal from the much weaker methyl loss channel of the D1-ethynyl–propylene reaction. Since the major goal is to explore molecular mass growth processes, we therefore focus on the atomic hydrogen loss of the ethynyl–propylene reaction. The next major hydrogen loss products predicted are *cis*- and *trans*-3-penten-1-yne (**p2** and **p3**) at overall levels of typically 26%–33% of all products; this corresponds to levels of up to 51% of all hydrogen loss products. This is followed by the 4-penten-1-yne product isomers (**p4–p6**) at 7%–9%, 7%–9%, and 6%–8%,

respectively. Recall that, within our signal-to-noise, which, for the present system, limits the detection of hydrogen versus deuterium losses to fractions above typically 10%, **p4–p6** were predicted to be minor products. Finally, the 3-methyl-3-buten-1-yne (**p9**) product is predicted to form in lower amounts than **p4–p6**, at levels of 3%–5%. The hydrogen loss channel leading to the thermodynamically most stable isomer, cyclopentadiene (**p7**), is predicted to contribute only 0.1% and has a reaction energy that lies outside our experimentally derived values.

Note that previous crossed-beam experiments on the reactions of propylene with small molecules/radicals have been conducted, namely, propylene with atomic carbon (C; ³P_j),⁵¹ dicarbon (C₂; X¹Σ_g⁺/a³Π_u),⁵² cyano (CN; X²Σ⁺),¹⁷ and methylidyne (CH; X²Π);⁵³ a comparison of these reaction products with the current study is presented in Scheme 2. In all

Scheme 2. Products Formed in the Bimolecular Reactions of Propylene with Small Carbon-Containing Reactants Such as Atomic Carbon (C; ³P_j), Dicarbon (C₂; X¹Σ_g⁺/a³Π_u), Cyano (CN; X²Σ⁺), Methylidyne (CH; X²Π), and Ethynyl (C₂H; X²Σ⁺) under Single Collision Conditions in Crossed Molecular Beam Experiments



five cases, the reaction is initiated by a barrierless addition; the carbon, dicarbon, and methylidyne reactants add to the double bond of propylene to form a cyclic three-member ring collision complex, while the cyano and ethynyl radicals add to the C1 and/or C2 carbon leading to an acyclic intermediate. In the methylidyne study, the ring structure remains intact upon atomic hydrogen loss decomposition, yielding 1- and 3-methylcyclopropene. Conversely, the initial intermediate in the reactions involving carbon and dicarbon undergoes ring opening before hydrogen atom loss to methylpropargyl (carbon–propylene) and 1- and 3-vinylpropargyl radicals (dicarbon–propylene). The cyano radical is isoelectronic to the ethynyl radical and, therefore, should have similar reaction dynamics.⁵⁴ The cyano radical adds to the C1 carbon of propylene forming the CH₃CHCH₂CN intermediate before H loss decomposition to *cis/trans*-2-butenitrile (75%) and 3-butenitrile (25%) at experimental reaction energies of -103 ± 8 kJ mol⁻¹. The ethynyl–propylene reaction follows the

equivalent pathway at experimental reaction energies of $-108 \pm 18 \text{ kJ mol}^{-1}$ through $\text{CH}_3\text{CHCH}_2\text{CCH}$ intermediates (**i3**/**i4**) before hydrogen loss to the major product *cis/trans*-3-penten-1-yne (**p2/p3**) with only a minor contribution to 4-penten-1-yne (**p4–p6**); these are isoelectronic to the *cis/trans*-2-butenenitrile and 3-butenenitrile products, respectively, formed from the cyano–propylene system. Notably, the five reactions are exoergic and all barriers have relative energies below that of the separated reactants, which indicates that these reactions can occur in cold interstellar environments such as molecular clouds.

5. CONCLUSION

Crossed molecular beams experiments were conducted to explore the chemical dynamics of the reaction of D1-ethynyl radicals (C_2D ; $\text{X}^2\Sigma^+$) with propylene (C_3H_6 ; $\text{X}^1\text{A}'$) and partially deuterated D3–3,3,3-propylene ($\text{C}_2\text{H}_3\text{CD}_3$; $\text{X}^1\text{A}'$). The reaction dynamics were inferred to be indirect and initiated by addition of the D1-ethynyl radical center to the C1 and/or C2 carbon of propylene yielding $\text{C}_3\text{H}_5\text{D}$ intermediate(s) before atomic hydrogen loss decomposition through a tight exit transition state. The combination of experimental results with the computed PES narrowed down the possible products to *cis/trans*-3-penten-1-yne (**p2/p3**) and 3-methyl-3-buten-1-yne (**p9**); out of these, RRKM calculations predict **p2** and **p3** as the major hydrogen loss products formed. Experiments utilizing D3–3,3,3-propylene are in agreement and help to eliminate nondominant reaction pathways to 4-penten-1-yne isomers (**p4–p6**). Although the ethynyl–propylene reaction does not lead to the cyclopentadiene molecule (*c*- C_5H_6 , X^1A_1), high-temperature environments such as circumstellar envelopes of carbon stars close to the central star, planetary nebulae as their descendants, as well as combustion systems may exhibit hydrogen-atom-assisted isomerization processes that could convert *cis/trans*-3-penten-1-yne and 3-methyl-3-buten-1-yne to cyclopentadiene (*c*- C_5H_6 , X^1A_1), similar to *trans*-1-phenylvinylacetylene and 4-phenylvinylacetylene isomerization to naphthalene.⁵⁵ The ethynyl radical and propylene have both been detected in the interstellar medium in cold molecular clouds like in TMC-1.^{11,14} Hence, based on the chemical dynamics derived, the title reaction should lead to *cis/trans*-3-penten-1-yne in cold interstellar environments such as TMC-1.

■ ASSOCIATED CONTENT

SI Supporting Information

The Supporting Information is available free of charge at <https://pubs.acs.org/doi/10.1021/acs.jpca.2c00297>.

Cartesian coordinates and vibrational frequencies (Table S1), as well as RRKM rate constants at 41.1 kJ mol^{-1} (Table S2) and 0 kJ mol^{-1} (Table S3) for all species on the potential energy surface (PDF)

■ AUTHOR INFORMATION

Corresponding Author

Ralf I. Kaiser – Department of Chemistry, University of Hawai'i at Mānoa, Honolulu, Hawaii 96822, United States; orcid.org/0000-0002-7233-7206; Email: ralfk@hawaii.edu

Authors

Shane J. Goettl – Department of Chemistry, University of Hawai'i at Mānoa, Honolulu, Hawaii 96822, United States
Chao He – Department of Chemistry, University of Hawai'i at Mānoa, Honolulu, Hawaii 96822, United States
Dababrata Paul – Department of Chemistry, University of Hawai'i at Mānoa, Honolulu, Hawaii 96822, United States
Anatoliy A. Nikolayev – Lebedev Physical Institute, Samara 443011, Russian Federation; Samara National Research University, Samara 443086, Russian Federation
Valeriy N. Azyazov – Lebedev Physical Institute, Samara 443011, Russian Federation; Samara National Research University, Samara 443086, Russian Federation
Alexander M. Mebel – Department of Chemistry and Biochemistry, Florida International University, Miami, Florida 33199, United States; orcid.org/0000-0002-7233-3133

Complete contact information is available at: <https://pubs.acs.org/doi/10.1021/acs.jpca.2c00297>

Notes

The authors declare no competing financial interest.

■ ACKNOWLEDGMENTS

This work was supported by the U.S. Department of Energy, Basic Energy Sciences (Grant Nos. DE-FG02-03ER15411 and DE-FG02-04ER15570) to the University of Hawaii and Florida International University, respectively. The work at Lebedev Physical Institute was supported by the Ministry of Higher Education and Science of the Russian Federation, under Grant No. 075-15-2021-597.

■ REFERENCES

- (1) Parker, D. S. N.; Mebel, A. M.; Kaiser, R. I. The role of isovalency in the reactions of the cyano (CN), boron monoxide (BO), silicon nitride (SiN), and ethynyl (C_2H) radicals with unsaturated hydrocarbons acetylene (C_2H_2) and ethylene (C_2H_4). *Chem. Soc. Rev.* **2014**, *43*, 2701.
- (2) Lockyear, J. F.; Fournier, M.; Sims, I. R.; Guillemin, J.-C.; Taatjes, C. A.; Osborn, D. L.; Leone, S. R. Formation of fulvene in the reaction of C_2H with 1,3-butadiene. *Int. J. Mass Spectrom.* **2015**, *378*, 232.
- (3) Turner, A. M.; Kaiser, R. I. Exploiting photoionization reflectron time-of-flight mass spectrometry to explore molecular mass growth processes to complex organic molecules in interstellar and solar system ice analogs. *Acc. Chem. Res.* **2020**, *53*, 2791.
- (4) Zhang, F.; Parker, D.; Kim, Y. S.; Kaiser, R. I.; Mebel, A. M. On the formation of ortho-benzynes (*o*- C_6H_4) under single collision conditions and its role in interstellar chemistry. *Astrophys. J.* **2011**, *728*, 141.
- (5) Cernicharo, J.; Agúndez, M.; Kaiser, R. I.; Cabezas, C.; Tercero, B.; Marcelino, N.; Pardo, J. R.; De Vicente, P. Discovery of benzyne, *o*- C_6H_4 , in TMC-1 with the QUIJOTE line survey. *Astron. Astrophys.* **2021**, *652*, L9.
- (6) Jones, B. M.; Zhang, F.; Kaiser, R. I.; Jamal, A.; Mebel, A. M.; Cordiner, M. A.; Charnley, S. B. Formation of benzene in the interstellar medium. *Proc. Natl. Acad. Sci. U. S. A.* **2011**, *108*, 452.
- (7) Dangi, B. B.; Parker, D. S. N.; Kaiser, R. I.; Jamal, A.; Mebel, A. M. A combined experimental and theoretical study on the gas-phase synthesis of toluene under single collision conditions. *Angew. Chem., Int. Ed.* **2013**, *52*, 7186.
- (8) Kaiser, R. I.; Stahl, F.; Schleyer, P. v. R.; Schaefer, H. F., III Atomic and molecular hydrogen elimination in the crossed beam reaction of d1-ethynyl radicals C_2D ($\text{X}^2\Sigma^+$) with acetylene, C_2H_2

- ($X^1\Sigma_g^+$): Dynamics of d1-diacetylene (HCCCCD) and d1-butadiynyl (DCCCC) formation. *Phys. Chem. Chem. Phys.* **2002**, *4*, 2950.
- (9) Gu, X.; Kim, Y. S.; Kaiser, R. I.; Mebel, A. M.; Liang, M. C.; Yung, Y. L. Chemical dynamics of triacetylene formation and implications to the synthesis of polyynes in Titan's atmosphere. *Proc. Natl. Acad. Sci. U. S. A.* **2009**, *106*, 16078.
- (10) Mebel, A. M.; Kislov, V. V.; Kaiser, R. I. Photoinduced mechanism of formation and growth of polycyclic aromatic hydrocarbons in low-temperature environments via successive ethynyl radical additions. *J. Am. Chem. Soc.* **2008**, *130*, 13618.
- (11) Tucker, K. D.; Kutner, M. L.; Thaddeus, P. The ethynyl radical C_2H - A new interstellar molecule. *Astrophys. J.* **1974**, *193*, L115.
- (12) Heays, A. N.; Bosman, A. D.; van Dishoeck, E. F. Photodissociation and photoionisation of atoms and molecules of astrophysical interest. *Astron. Astrophys.* **2017**, *602*, A105.
- (13) Chastaing, D.; James, P. L.; Sims, I. R.; Smith, I. W. M. Neutral-neutral reactions at the temperatures of interstellar clouds: Rate coefficients for reactions of C_2H radicals with O_2 , C_2H_2 , C_2H_4 and C_3H_6 down to 15 K. *Faraday Discuss.* **1998**, *109*, 165.
- (14) Marcelino, N.; Cernicharo, J.; Agúndez, M.; Roueff, E.; Gerin, M.; Martín-Pintado, J.; Mauersberger, R.; Thum, C. Discovery of interstellar propylene (CH_2CHCH_3): Missing links in interstellar gas-phase chemistry. *Astrophys. J., Lett.* **2007**, *665*, L127.
- (15) Nixon, C. A.; Jennings, D. E.; Bezaud, B.; Vinatier, S.; Teanby, N. A.; Sung, K.; Ansty, T. M.; Irwin, P. G. J.; Goriunov, N.; Cottini, V.; et al. Detection of propene in Titan's stratosphere. *Astrophys. J., Lett.* **2013**, *776*, L14.
- (16) Cernicharo, J.; Agúndez, M.; Cabezas, C.; Tercero, B.; Marcelino, N.; Pardo, J. R.; de Vicente, P. Pure hydrocarbon cycles in TMC-1: Discovery of ethynyl cyclopropenylidene, cyclopentadiene, and indene. *Astron. Astrophys.* **2021**, *649*, L15.
- (17) Gu, X.; Zhang, F.; Kaiser, R. I. Reaction dynamics on the formation of 1-and 3-cyanopropylene in the crossed beams reaction of ground-state cyano radicals (CN) with propylene (C_3H_6) and its deuterated isotopologues. *J. Phys. Chem. A* **2008**, *112*, 9607.
- (18) Gu, X.; Guo, Y.; Kaiser, R. I. Mass spectrum of the butadiynyl radical (C_4H ; $X^2\Sigma^+$). *Int. J. Mass Spectrom.* **2005**, *246*, 29.
- (19) Goettl, S. J.; Doddipatla, S.; Yang, Z.; He, C.; Kaiser, R. I.; Silva, M. X.; Galvão, B. R. L.; Millar, T. J. Chemical dynamics study on the gas-phase reaction of the D1-silyldiyne radical (SiD; $X^2\Pi$) with deuterium sulfide (D_2S) and hydrogen sulfide (H_2S). *Phys. Chem. Chem. Phys.* **2021**, *23*, 13647.
- (20) Gu, X.; Guo, Y.; Kawamura, E.; Kaiser, R. I. Characteristics and diagnostics of an ultrahigh vacuum compatible laser ablation source for crossed molecular beam experiments. *J. Vac. Sci. Technol., A* **2006**, *24*, 505.
- (21) Guo, Y.; Gu, X.; Kawamura, E.; Kaiser, R. I. Design of a modular and versatile interlock system for ultrahigh vacuum machines: A crossed molecular beam setup as a case study. *Rev. Sci. Instrum.* **2006**, *77*, 034701.
- (22) Guo, Y.; Gu, X.; Kaiser, R. I. Mass spectrum of the 1-butene-3-yne-2-yl radical ($i-C_4H_3$; X^2A'). *Int. J. Mass Spectrom.* **2006**, *249*, 420.
- (23) Thomas, A. M.; Dangi, B. B.; Yang, T.; Kaiser, R. I.; Sun, B.-J.; Chou, T.-J.; Chang, A. H. H. A crossed molecular beams investigation of the reactions of atomic silicon (Si (3P)) with C_4H_6 isomers (1, 3-butadiene, 1, 2-butadiene, and 1-butyne). *Chem. Phys.* **2019**, *520*, 70.
- (24) Gu, X.; Kaiser, R. I.; Mebel, A. M.; Kislov, V. V.; Klippenstein, S. J.; Harding, L. B.; Liang, M.-C.; Yung, Y. L. A crossed molecular beams study on the formation of the exotic cyanoethynyl radical in Titan's atmosphere. *Astrophys. J.* **2009**, *701*, 1797.
- (25) Guo, Y.; Gu, X.; Balucani, N.; Kaiser, R. I. Formation of the 2,4-pentadiynyl-1 radical ($H_2CCCCCH$, X^2B_1) in the crossed beams reaction of dicarbon molecules with methylacetylene. *J. Phys. Chem. A* **2006**, *110*, 6245.
- (26) Balucani, N.; Mebel, A. M.; Lee, Y. T.; Kaiser, R. I. A combined crossed molecular beam and ab initio study of the reactions $C_2(X^1\Sigma_g^+, a^3\Pi_u) + C_2H_4 \rightarrow n-C_4H_3(X^2A') + H(^2S_{1/2})$. *J. Phys. Chem. A* **2001**, *105*, 9813.
- (27) Kaiser, R. I.; Balucani, N.; Charkin, D. O.; Mebel, A. M. A crossed beam and ab initio study of the $C_2(X^1\Sigma_g^+/a^3\Pi_u) + C_2H_2(X^1\Sigma_g^+)$ reactions. *Chem. Phys. Lett.* **2003**, *382*, 112.
- (28) Kaiser, R. I.; Chiong, C. C.; Asvany, O.; Lee, Y. T.; Stahl, F.; Schleyer, P. v. R.; Schaefer, H. F., III. Chemical dynamics of D1-methyldiacetylene (CH_3CCCCD ; X^1A_1) and d1-ethynylallene ($H_2CCCH(C_2D)$; X^1A') formation from reaction of $C_2D(X^2\Sigma^+)$ with methylacetylene, $CH_3CCH(X^1A_1)$. *J. Chem. Phys.* **2001**, *114*, 3488.
- (29) Proch, D.; Trickl, T. A high-intensity multi-purpose piezoelectric pulsed molecular beam source. *Rev. Sci. Instrum.* **1989**, *60*, 713.
- (30) Stahl, F.; Schleyer, P. v. R.; Bettinger, H. F.; Kaiser, R. I.; Lee, Y. T.; Schaefer, H. F., III. Reaction of the ethynyl radical, C_2H , with methylacetylene, CH_3CCH , under single collision conditions: Implications for astrochemistry. *J. Chem. Phys.* **2001**, *114*, 3476.
- (31) Stahl, F.; Schleyer, P. v. R.; Schaefer, H. F., III; Kaiser, R. I. Reactions of ethynyl radicals as a source of C_4 and C_5 hydrocarbons in Titan's atmosphere. *Planet. Space Sci.* **2002**, *50*, 685.
- (32) Gu, X.; Guo, Y.; Mebel, A. M.; Kaiser, R. I. A crossed beam investigation of the reactions of tricarbon molecules, $C_3(X^1\Sigma_g^+)$, with acetylene, $C_2H_2(X^1\Sigma_g^+)$, ethylene, $C_2H_4(X^1A_g)$, and benzene, $C_6H_6(X^1A_{1g})$. *Chem. Phys. Lett.* **2007**, *449*, 44.
- (33) Guo, Y.; Gu, X.; Zhang, F.; Mebel, A. M.; Kaiser, R. I. A crossed molecular beam study on the formation of hexenediynyl radicals ($H_2CCCCCCH$; $C_6H_3(X^2A')$) via reactions of tricarbon molecules, $C_3(X^1\Sigma_g^+)$, with allene (H_2CCCH_2 ; X^1A_1) and methylacetylene (CH_3CCH ; X^1A_1). *Phys. Chem. Chem. Phys.* **2007**, *9*, 1972.
- (34) Vernon, M. F. *Molecular Beam Scattering*. Ph.D. Dissertation, University of California at Berkeley, 1983.
- (35) Weiss, P. S. *Reaction Dynamics of Electronically Excited Alkali Atoms with Simple Molecules*. Ph.D. Dissertation, University of California at Berkeley, 1985.
- (36) Kaiser, R. I. Experimental investigation on the formation of carbon-bearing molecules in the interstellar medium via neutral-neutral reactions. *Chem. Rev.* **2002**, *102*, 1309.
- (37) Chai, J.-D.; Head-Gordon, M. Long-range corrected hybrid density functionals with damped atom-atom dispersion corrections. *Phys. Chem. Chem. Phys.* **2008**, *10*, 6615.
- (38) Adler, T. B.; Knizia, G.; Werner, H.-J. A simple and efficient CCSD (T)-F12 approximation. *J. Chem. Phys.* **2007**, *127*, 221106.
- (39) Knizia, G.; Adler, T. B.; Werner, H.-J. Simplified CCSD(T)-F12 methods: Theory and benchmarks. *J. Chem. Phys.* **2009**, *130*, 054104.
- (40) Dunning, T. H., Jr. Gaussian basis sets for use in correlated molecular calculations. I. The atoms boron through neon and hydrogen. *J. Chem. Phys.* **1989**, *90*, 1007.
- (41) Zhang, J.; Valeev, E. F. Prediction of reaction barriers and thermochemical properties with explicitly correlated coupled-cluster methods: A basis set assessment. *J. Chem. Theory Comput.* **2012**, *8*, 3175.
- (42) Frisch, M. J.; Trucks, G. W.; Schlegel, H. B.; Scuseria, G. E.; Robb, M. A.; Cheeseman, J. R.; Scalmani, G.; Barone, V.; Mennucci, B.; Petersson, G. A. et al. *Gaussian 09*, Revision A.1; Gaussian, Inc.: Wallingford, CT, 2009.
- (43) Werner, H. J.; Knowles, P. J.; Lindh, R.; Manby, F. R.; Schütz, M.; Celani, P.; Korona, T.; Rauhut, G.; Amos, R. D.; Bernhardsson, A. *MOLPRO, a Package of Ab Initio Programs*, Version 2010.1; University of Cardiff: Cardiff, U.K., 2010.
- (44) Steinfeld, J. I.; Francisco, J. S.; Hase, W. L. *Chemical Kinetics and Dynamics*, Vol. 3; Prentice Hall: Englewood Cliffs, NJ, 1989.
- (45) Eyring, H.; Lin, S. H. *Basic Chemical Kinetics*; John Wiley & Sons, Inc.: New York, 1980.
- (46) Robinson, P. J.; Holbrook, K. A. *Unimolecular Reactions*; Wiley: New York, 1972.
- (47) He, C.; Zhao, L.; Thomas, A. M.; Morozov, A. N.; Mebel, A. M.; Kaiser, R. I. Elucidating the chemical dynamics of the elementary reactions of the 1-propynyl radical (CH_3CC ; X^2A_1) with methyl-

acetylene (H_3CCCH ; X^1A_1) and allene (H_2CCCH_2 ; X^1A_1). *J. Phys. Chem. A* **2019**, *123*, 5446.

(48) Kislov, V. V.; Nguyen, T. L.; Mebel, A. M.; Lin, S. H.; Smith, S. C. Photodissociation of benzene under collision-free conditions: An ab initio/Rice–Ramsperger–Kassel–Marcus study. *J. Chem. Phys.* **2004**, *120*, 7008.

(49) Safron, S. A.; Weinstein, N. D.; Herschbach, D. R.; Tully, J. C. Transition state theory for collision complexes: product translational energy distributions. *Chem. Phys. Lett.* **1972**, *12*, 564.

(50) Kaiser, R. I.; Lee, Y. T.; Suits, A. G. Crossed-beam reaction of carbon atoms with hydrocarbon molecules. I. Chemical dynamics of the propargyl radical formation, C_3H_3 (X^2B_2), from reaction of $\text{C}(^3P_1)$ with ethylene, C_2H_4 (X^1A_g). *J. Chem. Phys.* **1996**, *105*, 8705.

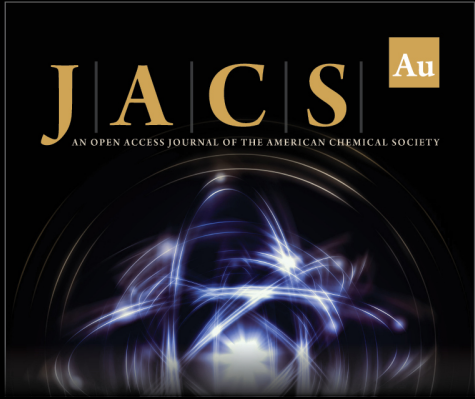
(51) Kaiser, R. I.; Stranges, D.; Bevsek, H. M.; Lee, Y. T.; Suits, A. G. Crossed-beam reaction of carbon atoms with hydrocarbon molecules. IV. Chemical dynamics of methylpropargyl radical formation, C_4H_5 , from reaction of $\text{C}(^3P_1)$ with propylene, C_3H_6 (X^1A). *J. Chem. Phys.* **1997**, *106*, 4945.

(52) Dangi, B. B.; Maity, S.; Kaiser, R. I.; Mebel, A. M. A combined crossed beam and ab initio investigation of the gas phase reaction of dicarbon molecules (C_2 ; $X^1\Sigma_g^+/a^3\Pi_u$) with propene (C_3H_6 ; X^1A'): identification of the resonantly stabilized free radicals 1-and 3-vinylpropargyl. *J. Phys. Chem. A* **2013**, *117*, 11783.

(53) He, C.; Thomas, A. M.; Galimova, G. R.; Mebel, A. M.; Kaiser, R. I. Gas-phase formation of 1-methylcyclopropene and 3-methylcyclopropene via the reaction of the methylidyne radical (CH ; $X^2\Pi$) with propylene (CH_3CHCH_2 ; X^1A'). *J. Phys. Chem. A* **2019**, *123*, 10543.

(54) Langmuir, I. The arrangement of electrons in atoms and molecules. *J. Am. Chem. Soc.* **1919**, *41*, 868.

(55) Zhao, L.; Kaiser, R. I.; Xu, B.; Ablikim, U.; Ahmed, M.; Zagidullin, M. V.; Azyazov, V. N.; Howlader, A. H.; Wnuk, S. F.; Mebel, A. M. VUV photoionization study of the formation of the simplest polycyclic aromatic hydrocarbon: Naphthalene (C_{10}H_8). *J. Phys. Chem. Lett.* **2018**, *9*, 2620.



JACS Au
AN OPEN ACCESS JOURNAL OF THE AMERICAN CHEMICAL SOCIETY

 Editor-in-Chief
Prof. Christopher W. Jones
Georgia Institute of Technology, USA

Open for Submissions 

pubs.acs.org/jacsau  ACS Publications
Most Trusted. Most Cited. Most Read.